Published in final edited form as:
Psychopharmacology (Berl). 2011 April ; 214(3): 707–718. doi:10.1007/s00213-010-2076-4.

Inhibitory effects of alcohol on glucose transport across the blood–brain barrier leads to neurodegeneration: preventive role of acetyl-L-carnitine

P. M. Abdul Muneer, **Saleena Alikunju**, **Adam M. Szlachetka**, and **James Haorah**
Laboratory of Neurovascular Oxidative Injury, Department of Pharmacology and Experimental Neuroscience, University of Nebraska Medical Center, Omaha, NE 68198, USA

Abstract

Purpose—Evidence shows that alcohol intake causes oxidative neuronal injury and neurocognitive deficits that are distinct from the classical Wernicke-Korsakoff neuropathy. Our previous findings indicated that alcohol-elicited blood-brain barrier (BBB) damage leads to neuroinflammation and neuronal loss. The dynamic function of the BBB requires a constant supply and utilization of glucose. Here we examined whether interference of glucose uptake and transport at the endothelium by alcohol leads to BBB dysfunction and neuronal degeneration.

Material and methods—We tested the hypothesis in cell culture of human brain endothelial cells, neurons and alcohol intake in animal by immunofluorescence, Western blotting and glucose uptake assay methods.

Results—We found that decrease in glucose uptake correlates the reduction of glucose transporter protein 1 (GLUT1) in cell culture after 50 mM ethanol exposure. Decrease in GLUT1 protein levels was regulated at the translation process. In animal, chronic alcohol intake suppresses the transport of glucose into the frontal and occipital regions of the brain. This finding is validated by a marked decrease in GLUT1 protein expression in brain microvessel (the BBB). In parallel, alcohol intake impairs the BBB tight junction proteins occludin, zonula occludens-1, and claudin-5 in the brain microvessel. Permeability of sodium fluorescein and Evans Blue confirms the leakiness of the BBB. Further, depletion of trans-endothelial electrical resistance of the cell monolayer supports the disruption of BBB integrity. Administration of acetyl-L-carnitine (a neuroprotective agent) significantly prevents the adverse effects of alcohol on glucose uptake, BBB damage and neuronal degeneration.

Conclusion—These findings suggest that alcohol-elicited inhibition of glucose transport at the blood-brain interface leads to BBB malfunction and neurological complications.

Keywords

Blood–brain barrier; Glucose transporter protein; Trans-endothelial electrical resistance; Acetyl-L-carnitine; Tight junction; Neurodegeneration

jhaorah@unmc.edu .

Conflict of interest The authors declare that they have no conflict of interest.

Introduction

Alcohol is the most commonly used and abused drug that accounts for more than 100,000 deaths and 297,000 disfigured persons each year. About 20 million people are alcoholics or alcohol abusers in the USA (WHO 2007). Chronic alcohol abusers suffer from neurocognitive deficits, neuronal injury, and neuronal loss (Harper 1998;Parsons 1998;Zeigler et al. 2005). Although the central nervous system is a major target of alcohol for causing metabolic and neurological disorders (Oscar-Berman and Marinkovic 2003), the exact mechanism of such neuro-degeneration remains unclear. There is strong evidence that neurological disease like Alzheimer's, Parkinson's, and stroke are resulted from mitochondrial oxidative damage (Lin and Beal 2006;Maracchioni et al. 2007). In alcohol consumption, the role of mitochondrial oxidative damage has been demonstrated in alcoholic liver damage (Bailey et al. 1999;Cahill et al. 2002;Kessova and Cederbaum 2007;Pastorino et al. 1999) and in neuronal degeneration (Haorah et al. 2008a;Rump et al. 2010). These findings therefore suggest the role of oxidative damage and imbalanced bioenergy homeostasis for neuronal loss and neurological complications. That is because mitochondria are the “power house” and the “oxidative phosphorylation” organelle center for operating the cellular and organ function. In chronic alcohol abuse, Wernicke–Korsakoff neuropathy is an example of energy metabolic disorder syndrome where deficiency of thiamine (a co-factor for pyruvate dehydrogenase) impairs the conversion of pyruvate to acetylcoenzyme A, resulting in pathogenesis (Harper 1998;Harper et al. 2003).

The brain cells derive 90% of the energy requirements from glucose metabolism (Handa et al. 2000). Therefore, disruption of glucose uptake and utilization in the brain is expected to cause adverse effects on the function and survival of the brain cells. It has been reported that acute ethanol exposure significantly reduces the uptake and utilization of glucose by rat fetal astrocytes culture (Singh et al. 2006). Interestingly, acute administration of ethanol decreases the levels of glucose transporter protein 1 (GLUT1) and GLUT3 in protein extracts from cortical plasma membrane without affecting glucose uptake and utilization in rat brain (Handa et al. 2000). Recent work by Volkow et al. (2006) measures the metabolism of glucose in different regions of the brain by positron emission tomography using 2-deoxy-2-[^{18}F]fluoro-D-glucose in alcoholics (Volkow et al. 2006). Findings from these studies indicate a decline glucose metabolism in the frontal cortex of chronic alcohol abusers but with a significant increase in glucose metabolism during alcohol withdrawal period. These studies clearly show that alcohol negatively interferes with glucose uptake and utilization in the brain.

The rate-limiting factor for glucose transport into the brain is expected to dependent on blood glucose concentration and transporter protein at the blood–brain barrier (BBB) interface. Therefore, disruption of BBB integrity may also hamper the uptake and transport of glucose into the brain. We have shown that alcohol exposure alters the permeability of biomarkers and migration of monocytes across the BBB via oxidative stress-mediated disruption of the interface (Haorah et al. 2005b, 2007b). We previously demonstrated that this alcohol-induced loss of BBB integrity is regulated by activation of myosin light chain kinase (Haorah et al. 2005a), inositol 1,4,5-triphosphate-gated intracellular Ca^{2+} release (Haorah et al. 2007a), and protein tyrosine kinase-mediated matrix metalloproteinases signaling pathways (Haorah et al. 2008b). The purpose of the present study is to examine whether impairment of glucose uptake and transport at the interface contributes to alcohol-elicited BBB dysfunction and subsequent neuronal loss. At the BBB, the transport of glucose from the arterial vessel circulation into the brain is facilitated by GLUT1 (Leybaert 2005), which exists in highly glycosylated 55-kDa isoform and less glycosylated 45-kDa isoform (Maher et al. 1994; Yeh et al. 2008). Our study shows that GLUT1 55-kDa isoform is highly expressed in primary human brain endothelial cells (hBECs) as well as in mice

brain microvessel. We also examined the protective effect of acetyl-L-carnitine (ALC) on glucose uptake and transporter protein from the adverse effect of alcohol insults. ALC, a naturally occurring neuroprotective agent, is currently used for treatment of neurological diseases (Hagen et al. 1998, 2002; Lolic et al. 1997; Pettegrew et al. 1995).

Materials and methods

Reagents

We purchased the antibodies to GLUT1, neuro-filament (NF), tyrosine hydroxylase (TH), choline acetyltransferase (ChAT) from Abcam (Cambridge, MA, USA), antibodies to occludin, claudin-5 and ZO-1 from Zymed (Invitrogen, Carlsbad, CA, USA), and antibody to α-actin from Millipore (Billerica, MA, USA). All secondary Alexa Flour antibodies were purchased from Invitrogen. D-(2-^{3}H)-Glucose (5 mCi, 185 MBq) was purchased from PerkinElmer Life and Analytical Sciences (Waltham, MA, USA). Cytochalasin B (CB), cycloheximide (Chx), actinomycin D (act-D), and ALC were purchased from Sigma-Aldrich (St. Louis, MO, USA).

hBEC culture

Primary hBECs were obtained from Dr. Persidsky, Temple University School of Medicine, and hBECs were cultured as described previously (Haorah et al. 2007a). Briefly, all cell culture plates and glass cover slips were pre-coated with type 1 rat-tail collagen (0.09 mg/ml in double-distilled sterile water), aspirated the excess collagen, and dried the plates overnight in sterile hood. The cells were cultured on 96-well plates (20,000 cells/well) for glucose uptake and viability assays, for immunohistochemistry cells were plated on 12-well glass cover slips (40,000 cells/well), and for protein extractions cells were cultured in T 75-cm^2 flasks (1×10^6 cells/flask). Dulbecco's modified Eagle medium (DMEM)/F-12 media containing 10 mM Hepes, 13 mM sodium bicarbonate (pH 7), 10% fetal bovine serum, penicillin, and streptomycin (100 μg/ml each, Invitrogen) was used for cell culture. Cell culture media were changed every 3 days until tight monolayers were formed in about 6–8 days.

Neuronal culture

Cortical neurons were obtained from our neural tissue core facility, where routinely isolated these cells from elective abortus specimens of human fetal brain tissue. Tissues were obtained in full compliance with the ethical guidelines of both the National Institutes of Health (NIH) and the University of Nebraska. Briefly, dissociated tissues were incubated with 0.25% trypsin for 30 min, neutralized with 10% fetal bovine serum, and further dissociated by trituration. Neurons were cultured on poly-D-lysine pre-coated cover slips and flasks (BD Labware, Bedford, MA, USA) in Neurobasal™ medium containing 0.5 mM glutamine, 50 μg/ml each of penicillin, and streptomycin in combination with GIBCO™ B-27 supplement with antioxidants as described previously (Haorah et al. 2008b). Purity of neurons was assessed by MAP-2 Abs (Chemicon), resulting in 100% enrichment of neurons. Neurons were plated on 12-well glass cover slips (40,000 cells/well), and cell culture media were changed every 3 days until 12–14 days.

In vitro glucose uptake

D-(2-^{3}H)-Glucose uptake was performed in hBECs cultured in 96-well plates following the modified method of Takakura et al. (1991). Cells were exposed to 50 mM ethanol (EtOH) for 24 h with or without 10 μM cytochalasin B, an inhibitor of glucose transporter protein (CB, 10 mM stock was dissolved in dimethyl sulfoxide), or 200 μM ALC in a CO_2 incubator. Cells were incubated overnight in glucose-free DMEM/F-12 media containing 2.0

μCi of D-(2-^{3}H)-glucose (specific activity=20–30 Ci/mmol) and 2.0 mM of non-radiolabeled glucose. After washing off the excess ^{3}H-glucose with phosphate saline buffer (PBS), cellular protein was precipitated with 10% trichloroacetic acid (TCA) at 4°C for 15 min. Following the manufacturer's instruction, precipitated proteins were transferred onto a 96-well nitrocellulose filter using the Unifilter-96 well Harvester (PerkinElmer, Waltham, MA, USA). Using the Beckman 96-well plate reader, radioactivity was measured by β-top counter. The concentrations of EtOH (50 mM) and CB (10 μM, specific inhibitor of GLUT) were derived from dose- and time-dependent toxicity assays (5–200 mM EtOH and 0.5–100 μM CB for 24–72 h), in which 50 mM EtOH or 10 μM of CB had no cell toxicity effect (by 3-(4,5-dimethylthiazol-2-yl)-2,5-diphenyltetrazolium bromide assay). The concentration of EtOH from 65 to 100 mM showed about 20% cell death after 48-h exposure. Concentration of CB higher than 20 μM was toxic to hBECs.

Analyses of GLUT1 protein and mRNA levels

Primary human brain endothelial cells cultured in rat-tail collagen and fibronectin pre-coated 75-cm^2 flasks were pre-incubated for 15 min with 100 ng/ml of act-D or 10 μg/ml of Chx (Sigma) prior to 16 h treatment with EtOH in the presence of act-D. Cell pellets were lyzed with ice-cold lysis buffer (50 mM Tris-Hcl, pH 7.5) containing 20% glycerol, 5 mM $MgCl_2$, 0.5 mM DTT, and protease inhibitor cocktail for protein extracts that were used for Western blot analyses of GLUT1 protein levels. Total cellular RNA was extracted from cell pellets by RNAeasy kit (Qiagen, Valencia, CA, USA) for GLUT1 mRNA levels. RNA was reverse-transcribed with random hexamers (Promega, Madison, WI, USA). Real-time quantitative PCR was performed with cDNA using an ABI PRISM 7000 sequence detector (Applied Biosystems, Foster City, CA, USA). Thermocy-cling conditions were 95°C for 10 min, 15 s, and 60°C for 1 min. Human-specific primer pairs for amplification of GLUT1 mRNA by quantitative reverse transcription polymerase chain reaction of total RNA were forward primer 5′-GAG TGC CTG AAA CCA GAG GA-3′ and the reverse primer 5′-CTC ACA CTT GGG AGT CA-3′. Human-specific primer pairs for glyceraldehyde 3-phosphate dehydrogenase (GAPDH) were forward primer: 5′-AAG GCC ATC ACC ATC TTC CA-3′ and reverse primer: 5′-ACC CCA CTT GAT GTT GG CA-3′. Using SYBR Green I detection system, a melting temperature dissociation curve was generated for the PCR product. All PCR reagents were obtained from Applied Biosystems (Foster City, CA, USA). Gene expression was normalized to GAPDH, used as an endogenous control.

Immunofluorescent detection

For immunocytochemistry, the hBECs were cultured on glass cover slips in 12-well flasks until 80–100% confluent. Cells were treated with 50 mM EtOH with and without CB (10 μM) or ALC (200 μM) for 24 h. Brain tissue sections (8 μm thickness) were derived from chronic EtOH, EtOH + ALC, or pair-fed control mice. Cells and tissue sections were washed with PBS; fixed in acetone–methanol (1:1 *v*/*v*) fixative; blocked the cellular antigen with 3% bovine serum albumin at room temperature for 1 h, in the presence of 0.4% Triton X-100; and incubated with respective primary antibodies such as mouse anti-GLUT1 (1:250 dilution), rabbit anti-von Willebrand factor (vWF; 1:150 dilution), rabbit anti-NF (Abcam, 1:250), sheep anti-TH (Abcam, 1:1,000 dilution), and rabbit anti-ChAT (Abcam, 1:100 dilution) for overnight at 4°C. After washing with PBS, cells and tissues were incubated for 1 h with secondary antibody: anti-mouse IgG Alexa Flour 488 for GLUT1, anti-rabbit-IgG Alexa Flour 594 for vWF, anti-rabbit IgG Alexa Flour 488 for NF, anti-sheep IgG Alexa Flour 488 for TH, and anti-rabbit IgG Alexa Flour 488 for ChAT. Cover slips were then mounted onto glass slides with immunomount containing DAPI (Invitrogen), and fluorescence microphotographs were captured by fluorescent microscopy (Eclipse TE2000-U, Nikon microscope, Melville, NY, USA) using NIS elements (Nikon, Melville, NY, USA)

software. GLUT1 expression was also analyzed in brain microvessels that were surgically dissected under microscope.

Western blot

The hBECs cultured in T 75-cm^2 flasks were lysed with CellLytic-M buffer (Sigma) for 30 min at 4°C, centrifuged at 1,4000×g, and then total cell lysates protein concentrations were estimated by bicinchoninic acid (Thermo Scientific, Rockford, IL, USA). We loaded 20-μg protein/lane and resolved the various molecular weight proteins by sodium dodecyl sulfate polyacrylamide gel electrophoresis on gradient gels (Thermo Scientific) and then transferred the protein onto nitrocellulose membranes. After blocking, membranes were incubated for overnight with primary antibodies against mouse GLUT1 (1:1,000, Abcam, Cambridge, MA, USA), rabbit occludin (1:250), mouse claudin-5 (1:1,000), and rabbit ZO-1 (1:250) at 4°C followed by 1 h incubation with horseradish peroxidase-conjugated secondary antibodies. Immunoreactive bands were detected by West Pico chemiluminescence substrate (Thermo Scientific). Data were quantified as arbitrary densitometry intensity units using the Gelpro32 software package (Version 3.1, Media Cybernetics, Marlow, UK).

In vivo glucose transport assay

Five-week-old C57BL/6J male mice from Jackson Laboratory (Bar Harbor, ME, USA) were housed in University of Nebraska Medical Center animal facility following NIH Guide for Care and Use of Laboratory Animals. Mice were acclimated to Lieber–DeCarli control and 28% calorie (4% vol/vol) ethanol liquid diets from Dyets Inc. for 5 days prior to 8- to 9-week weight-match pair-feeding regimens. Pair feeding was based on the amount of liquid diets consumed by ethanol group animals. In mouse model, 4% ethanol is considered as moderately high alcohol concentration; thus, in this study, the effects of ethanol on glucose transport and BBB function referred to high-dose chronic effects. ALC (1.0 mg/ml) was given daily in liquid diets mixture for 8 to 9 weeks. Experimental conditions consisted of control liquid diets, EtOH liquid diets, ALC in EtOH liquid diets, and ALC in control liquid diets. After week 8 of liquid-diet feeding, D-(2-^{3}H)-glucose (4 μCi) and 4.0 mM non-radiolabeled glucose in 500 μl of saline were cavaged orally for control, EtOH, and EtOH + ALC animals. After 1 h, mice were euthanized, microvessels were removed carefully, and tissues were dissected from different brain regions. Known tissue weights were homogenized with 100 μl of Krebs–Ringer phosphate HEPES buffer, centrifuged at 12,000 rpm for 15 min, and 20 μl of supernatants from each condition was mixed with 4 ml of scintillation fluid. The levels of ^{3}H-glucose in the samples were detected by liquid scintillation counter (Beckman) along with a standard curve of ^{3}H-glucose that was run in parallel. Results were extrapolated from the standard curve, and data were expressed as nanocurie per gram tissue weight.

In vivo BBB permeability assay

Using the sodium fluorescein (NaFl) and Evans Blue (EB) tracer dye mixtures (5 μM each), the effect of EtOH on BBB permeability was examined in acute and chronic animal model following an established method (Hawkins and Egleton 2006). In acute studies, mice were anesthetized, infused 100 μlof200 μM of ALC or 650 mM of EtOH through the common carotid artery for 1 h, and followed by infusion of NaFl/EB mixtures for another 30 min. ALC was infused at 30 min prior to EtOH infusion. In chronic studies, the conditions of control, EtOH, and EtOH + ALC were same as that of glucose uptake assay. Mixtures of NaFl/EB dyes were directly infused into the right carotid artery. Animals were decapitated; brains were removed, dissected, weighed, and homogenized in 600 μl 7.5% (*w*/*v*) TCA. Resulting suspensions were divided into two aliquots (300 μl each). One aliquot was neutralized with 50 μl of 5 N NaOH and measured by flourimetry on a GENios microplate reader (excitation 485 nm, emission 535 nm) for NaFl determination. The other aliquot was

centrifuged for 10 min at 10,000 rpm 4°C, and the supernatant was measured by absorbance spectroscopy at 620 nm for EB determination. Standard curve was constructed by serial dilutions of a standard EB/NaFl solution in 7.5% TCA.

TEER measurement

To determine the integrity of BBB function, changes in trans-endothelial electrical resistance (TEER) across the BBB were analyzed by a highly sensitive 1600R ECIS system (Applied Biophysics, Troy, NY, USA). The ECIS system provides real-time monitoring of changes in TEER. In brief, hBECs at 20,000 cells/well were plated on type I rat-tail collagen-coated 8W10E electrode arrays (Applied Biophysics). Once tight cell monolayers were formed, stable TEER readings were monitored for 2 h prior to treatment of cell monolayers with 50 and 100 mM EtOH in the presence or absence of CB or ALC. We then monitored the TEER readings for another 10 h at 400 Hz and with 10-min intervals. Confluent cell monolayers demonstrated baseline TEER readings of 1,100 to 1,200 Ω/cm^2.

Statistical analysis

Values are expressed as the mean ± SD. Within an individual experiment, each data point was determined from three to five replicates. Statistical analysis of the data was performed by using GraphPad Prism V5 (Sorrento Valley, CA, USA). Comparisons between samples were performed by one-way ANOVA with Dunnett's post hoc test. Differences were considered significant at P values ≤0.05.

Results

Ethanol inhibits glucose uptake and GLUT1 expression in hBECs

Primary hBECs were exposed to 50 mM of EtOH for 24 h. Then we assessed the changes in glucose uptake by ^{3}H-glucose labeled assay and GLUT1 expression by immunocytochemistry and Western blot analyses. Figure 1a–c shows that 50 mM EtOH significantly decreased glucose uptake and GLUT1 protein expression in hBECs. The reduction in glucose uptake and GLUT1 protein levels after EtOH exposure were prevented by ALC while glucose transporter protein inhibitor, CB, exacerbated the inhibitory effect of EtOH in hBECs (Fig. 1a–c). CB was used here to indicate the direct involvement of GLUT1 in hBECs for glucose uptake. Figure 1a showed a significant reduction (p<0.01) of glucose uptake in EtOH + CB compared with EtOH alone. Addition of CB to EtOH condition significantly exacerbated the reduction of glucose uptake (p<0.01) because CB is a specific inhibitor of GLUT. We also noted that unlike the results of glucose uptake, the presence of CB did not exacerbate the decrease in EtOH-elicited GLUT1 protein level because CB can only block the active binding sites of GLUT1 without affecting the degradation of GLUT1 protein as shown in Fig. 1b. The glucose uptake data and GLUT1 protein levels were supported by immunocytochemical detection of GLUT1 (Fig. 1d). Co-localization of GLUT1 with vWF confirmed the distribution of GLUT1 protein in hBECs. These results suggested that ALC safeguarded glucose uptake by stabilizing GLUT1 protein from deleterious effects of EtOH at the BBB. We attempted to explain the regulatory mechanisms for reduction of GLUT1 protein by exposing cultured hBECs to EtOH with/without a transcription inhibitor act-D (100 ng/ml) and a translation inhibitor Chx (10 μg/ml). Our results indicated that reduction in GLUT1 protein levels was regulated at the translation process since Chx + EtOH decreased the levels of GLUT1 protein and act-D did not alter the levels of GLUT1 protein (Fig. 2a, b). To confirm whether stabilization of GLUT1 mRNA levels by EtOH contributed to unchanged GLUT1 protein level, we quantified the mRNA levels by real-time quantitative polymerase chain reaction technique. Our results showed that EtOH did stabilize the GLUT1 mRNA level from the effect of act-D, while EtOH alone did not affect GLUT1 mRNA levels (Fig. 2c).

ALC protects glucose uptake in animal model

We then studied the glucose transport across the BBB in animal model as described in "Materials and methods". We observed that chronic EtOH administration significantly inhibited the transport of glucose across the BBB into the brain cerebral and cerebellum regions compared with the brain regions from controls (Fig. 3a, b). Interestingly, the inhibitory effect of alcohol on glucose transport across the blood–brain interface was prevented co-administration of ALC in liquid diets. To explain the molecular mechanisms of glucose transport impairment at the interface in chronic alcohol consumption, we analyzed the GLUT1 protein localization in brain microvessel by immunohistochemistry and GLUT1 protein content in protein extract from brain microvessel homogenate by Western blot. Our data indicate that GLUT1 protein was highly localized in control brain vessels that in turn co-localized well with the brain endothelial cell marker, vWF (Fig. 4a, b). However, chronic alcohol intake markedly decreased GLUT1 expression in brain vessels that correlated well with the diminished rate of glucose uptake by the BBB endothelium (Fig. 4c, d). Also, alcohol-elicited diminution in GLUT1 protein expression was effectively protected by ALC compared with chronic EtOH intake (Fig. 4e, f). We also determined the changes in GLUT1 expression in protein extracts from microvessel homogenates by Western blot analyses. In agreement with the data of GLUT1 expression, we also found that ALC protected the 55-kDa GLUT1 immunore-active protein bands from the adverse effects of chronic alcohol insults (Fig. 4g, h). In brain microvessel, the less glycosylated 45-kDa GLUT1 isoform was not detected, suggesting that localization of the highly glycosylated 55-kDa GLUT1 isoform was specific to the BBB. In the brain tissue section and tissue protein extracts, the 45 kDa was the prominent GLUT1 isoform with a very weak expression of 55-kDa isoform, which were both protected by ALC from chronic alcohol intake (Fig. 5a–h). The less glycosylated GLUT1 appeared to be co-localized well with astrocytic cell bodies in brain tissue section.

Disruption of glucose uptake impairs BBB integrity

We then evaluated whether impairment of glucose uptake and utilization in the brain endothelium contributed to malfunctioning of the BBB integrity. To study this, protein extracts from brain arterial vessels were analyzed for alterations of the BBB tight junction proteins such as occludin, ZO-1, and claudin-5 by Western blot. Our data revealed that reduction in occludin, ZO-1, and claudin-5 protein levels following chronic alcohol intake was significantly restored by co-administration of ALC in the liquid diets (Fig. 6a–c). The loss of BBB integrity was assessed by functional permeability of small molecular weight sodium fluorescein (NaFl) and large molecular weight EB markers across the blood–brain barrier. We noticed that increase in the permeability of NaFl and EB tracers across the BBB correlated with the disruption of BBB integrity in acute (Fig. 7a, b) as well as chronic (Fig. 7c, d) administration of ethanol compared with respective pair-fed control animals. Contamination of tracers in the brain was avoided by careful surgical removal of the microvessels from brain tissues. The protective effect of ALC was eminent by suppressing the EtOH-induced increase in BBB permeability of NaFl and EB tracers both in acute and in chronic conditions. Further, BBB dysfunction was assessed by alterations of the TEER of the brain endothelial cell monolayer, which monitored the tightness of the BBB. As expected, ethanol concentrations of 50 and 100 mM significantly reduced the electrical resistance of the cell monolayer dose-dependently (Fig. 7e). The presence of ALC was able to restore the effects of alcohol on TEER integrity. Cytochalasin B-mediated decrease in TEER suggests the importance of glucose uptake and utilization by brain endothelial cells for the maintenance of BBB integrity and barrier function.

BBB disruption promotes neuronal loss

Deficiency and impaired utilization of glucose in the brain as a result of BBB dysfunction was correlated with neurotoxicity in primary human neuronal culture and loss of neurons in

brain tissue sections. It was evident that ALC protected the integrity of neurofilaments from exposure to EtOH for 48 h (Fig. 8a–c) in neuronal culture. The treatment with CB for 48 h showed the neurodegeneration (data not shown), which suggests that glucose is inevitable for the survival of the brain cells. Primary human neuronal cells are very sensitive to ethanol concentration higher than 20 mM; therefore, a high concentration of 100 mM EtOH was used here to distinctly differentiate the protective effect of ALC. As a proof of concept, the loss of dopaminergic and cholinergic neurons was examined in the mid-cortex region of the whole brain tissue sections containing the hippocampus and striatum from chronic alcohol administration, pair-fed controls, and co-administration of ALC + EtOH. Brain cortical tissue sections from chronic alcohol ingestion showed a reduction in the number of dopaminergic neurons in the hippocampus and striatum area of the brain as indicated by TH (a marker for dopaminergic neurons) staining in Fig. 8d–f. Localization of ChAT staining (marker for cholinergic neurons) was more on the peripheral region of the brain surrounding the hippocampus and striatum area, which showed a diminished number of cholinergic neurons in alcohol intake compared with controls (Fig. 8g–i). Co-administration of ALC prevented the loss of dopaminergic and cholinergic neurons from alcohol. These findings suggest that inhibition of glucose uptake by brain endothelial cells plays a major role for BBB damage and subsequent neuronal degeneration.

Discussion

Glucose uptake, transport, and metabolism provide 90% of the energy in the brain under normal physiological condition. Since endothelial cells (primary cell component of BBB) regulate the delivery of glucose into the brain, the BBB endothelium plays a vital role for the supply of energy and nutrients to brain cells (Lund-Andersen et al. 1976). Thus, malfunctioning of the BBB is expected to adversely affect the uptake, transport, and utilization of glucose by different types of brain cells (neurons and glial cells) and their very survival. Our finding is the first to show that inhibitory effect of alcohol on glucose uptake and transport by brain endothelial cells causes BBB dysfunction and neuronal degeneration.

In the present study, the concentration of EtOH was determined from dose- and time-dependent effect on glucose uptake. Concentration of glucose was based on cellular glucose saturation uptake and that of cytochalasin B was determined by cell viability assay. Concentration of EtOH in chronic study was based on our animal model of ethanol liquid diets and pair-fed control. The concentration of glucose used in glucose-free media was justified by our cellular glucose saturation uptake study. Note that the cells were exposed EtOH but not starved with glucose; thus, the saturation of glucose uptake was less than 1.0 mM, which was within the 3.4 mM intracellular concentration of glucose in endothelial cells (Pardridge and Boado 1993).

The present findings show that alcohol significantly inhibited the uptake and transport of glucose across the BBB, in which the in vitro finding was validated by in vivo data. Decrease in glucose uptake in cells and glucose transport across the BBB in mice correlated with reduction of GLUT1 protein expression in cell culture and in brain microvessels. Clearly, ethanol decreased the levels of highly glycosylated 55-kDa GLUT1 protein in microvessel and the levels of the less glycosylated 45-kDa isoform in the brain. Co-localization of GLUT1 protein with astrocytes marker (glial fibrillar acidic protein) suggests that 45-kDa GLUT1 appeared to localize in the perivascular end-feet of astrocytes, similar to the findings of others (Maher et al. 1994; Yeh et al. 2008). Functionally, the 55-kDa GLUT1 is actively involved at the BBB for transport of glucose into the brain, whereas the 45-kDa GLUT1 is less active glucose transporter. This is because packaging of glucose into the transporter protein happens only when GLUT1 is glycosylated by acetylglucosamine. Since glycosylation of GLUT1 regulates the functional and structural integrity (Maher et al.

1994), it is possible that once the 55-kDa GLUT1 releases the glucose at the end-feet of astrocytes, it becomes less glycosylated and remains as 45-kDa isoform.

It was concluded that reduction in GLUT1 protein level was in part due to defective translocation of mRNA for biosynthesis of GLUT1 protein. This rationale was based on the similar effect of Chx, which inhibits protein synthesis by interfering the translocation of mRNA in the ribosomal reading frame. Treatment of cells with act-D did not affect the GLUT1 protein level (Fig. 2b), which was due to stabilization of GLUT1 mRNA levels by ethanol exposure. Interestingly, Boado (1998) showed that the brain-derived peptide preparation Cerebrolysin stabilizes the levels of GLUT1 mRNA in endothelial cells. Indeed, this is very similar to our previous findings that ethanol reduces the levels of insulin-like growth factor receptor II protein without affecting the IGFR II mRNA levels (Haorah et al. 2003).

Both in acute and in chronic conditions, alcohol negatively interferes the metabolism of glucose in the brain (Handa et al. 2000; Volkow et al. 2006). The question is whether the inhibitory effect of alcohol on glucose metabolism is due to inhibition of glucose transport at the BBB or the direct inhibition of glucose uptake by neurons and glial cells without affecting GLUT1 protein at the BBB. Our data suggest that inhibition of glucose transport across BBB by ethanol contributes to deprivation and defective metabolism of glucose in the brain. This notion is further supported by the fact that impairment of glucose uptake and GLUT1 protein expression in brain endothelium by alcohol is accompanied by breakdown of BBB integrity. That is because the dynamic function of the BBB is operated by a constant supply of glucose energy source. Therefore, alcohol-induced inhibition of endothelial glucose uptake is likely to disrupt the integrity of BBB function as well as the normal deliver of glucose into the brain leading to ultimate neurotoxicity and neuronal degeneration. Cytochalasin B, an inhibitor of GLUTs, decreased the rate of glucose uptake without affecting glucose transporters protein levels as indicated by immunocytochemistry and Western blot analyses. These results show that CB inhibited glucose uptake and transport by modulating the active binding sites of GLUTs and not by degrading the actual GLUTs protein contents.

The stabilization of glucose uptake, GLUT1 protein levels, and BBB integrity by ALC demonstrates the beneficial effect for improving the deleterious health condition of alcohol abusers. The complete penetration of ALC across the BBB (Kido et al. 2001) and our recent findings on neuroprotective mechanisms of ALC from alcohol-induced oxidative damage in the brain (Rump et al. 2010) strongly advocate the attractive therapeutic application for chronic alcohol abusers. ALC would stabilize glycosylation of GLUT1 protein by donating acetyl group to glucosamine so as to enhance the activity of acetylglucosamine, which glycosylates GLUT1 protein. Taken together, our findings indicate that ALC is a potent protective agent for neurological disorders.

In conclusion, our data suggest that EtOH-induced inhibition of glucose transport leads to BBB dysfunction, which fails to deliver adequate amount of glucose into the brain that exacerbates neurotoxicity and neuronal degeneration in vitro and in vivo. Further, therapeutic application of ALC would be beneficial for improving the health of EtOH abusers.

Acknowledgments

This work was supported in part by NIH/NIAAA grant AA016403-01A2 (to JH) and by University of Nebraska Medical Center Faculty Retention Fund. Primary human endothelial cells were kindly provided by Dr. Yuri Persidsky.

Abbreviations

ALC	Acetyl-L-carnitine
act-D	Actinomycin D
BBB	Blood–brain barrier
CB	Cytochalasin B
ChAT	Choline acetyltransferase
Chx	Cycloheximide
DMSO	Dimethyl sulfoxide
EB	Evans Blue
EtOH	Ethanol
GFAP	Glial fibrillar acidic protein
GLUT	Glucose transporter protein
hBECs	Human brain endothelial cells
MTT	3-(4,5-Dimethylthiazol-2-yl)-2,5-diphenyl-tetrazolium bromide
NaFl	Sodium fluorescein
NF	Neurofilament
TEER	Trans-endothelial electrical resistance
TH	Tyrosine hydroxylase
vWF	von Willebrand factor
ZO-1	Zonula occludens-1

References

Bailey SM, Pietsch EC, Cunningham CC. Ethanol stimulates the production of reactive oxygen species at mitochondrial complexes I and III. Free Radic Biol Med 1999;27:891–900. [PubMed: 10515594]

Boado RJ. Brain-derived peptides increase blood–brain barrier GLUT1 glucose transporter gene expression via mRNA stabilization. Neurosci Lett 1998;255:147–150. [PubMed: 9832194]

Cahill A, Cunningham CC, Adachi M, Ishii H, Bailey SM, Fromenty B, Davies A. Effects of alcohol and oxidative stress on liver pathology: the role of the mitochondrion. Alcohol Clin Exp Res 2002;26:907–915. [PubMed: 12068261]

Hagen TM, Ingersoll RT, Wehr CM, Lykkesfeldt J, Vinarsky V, Bartholomew JC, Song MH, Ames BN. Acetyl-L-carnitine fed to old rats partially restores mitochondrial function and ambulatory activity. Proc Natl Acad Sci USA 1998;95:9562–9566. [PubMed: 9689120]

Hagen TM, Liu J, Lykkesfeldt J, Wehr CM, Ingersoll RT, Vinarsky V, Bartholomew JC, Ames BN. Feeding acetyl-L-carnitine and lipoic acid to old rats significantly improves metabolic function while decreasing oxidative stress. Proc Natl Acad Sci USA 2002;99:1870–1875. [PubMed: 11854487]

Handa RK, DeJoseph MR, Singh LD, Hawkins RA, Singh SP. Glucose transporters and glucose utilization in rat brain after acute ethanol administration. Metab Brain Dis 2000;15:211–222. [PubMed: 11206590]

Haorah J, MacDonald RG, Stoner JA, Donohue TM Jr. Ethanol consumption decreases the synthesis of the mannose 6-phosphate/insulin-like growth factor II receptor but does not decrease its messenger RNA. Biochem Pharmacol 2003;65:637–648. [PubMed: 12566093]

Haorah J, Heilman D, Knipe B, Chrastil J, Leibhart J, Ghorpade A, Miller DW, Persidsky Y. Ethanol-induced activation of myosin light chain kinase leads to dysfunction of tight junctions and blood–brain barrier compromise. Alcohol Clin Exp Res 2005a;29:999–1009. [PubMed: 15976526]

Haorah J, Knipe B, Leibhart J, Ghorpade A, Persidsky Y. Alcohol-induced oxidative stress in brain endothelial cells causes blood–brain barrier dysfunction. J Leukoc Biol 2005b;78:1223–1232. [PubMed: 16204625]

Haorah J, Knipe B, Gorantla S, Zheng J, Persidsky Y. Alcohol-induced blood–brain barrier dysfunction is mediated via inositol 1, 4, 5-triphosphate receptor (IP3R)-gated intracellular calcium release. J Neurochem 2007a;100:324–336. [PubMed: 17241155]

Haorah J, Ramirez SH, Schall K, Smith D, Pandya R, Persidsky Y. Oxidative stress activates protein tyrosine kinase and matrix metalloproteinases leading to blood–brain barrier dysfunction. J Neurochem 2007b;101:566–576. [PubMed: 17250680]

Haorah J, Ramirez SH, Floreani N, Gorantla S, Morsey B, Persidsky Y. Mechanism of alcohol-induced oxidative stress and neuronal injury. Free Radic Biol Med 2008a;45:1542–1550. [PubMed: 18845238]

Haorah J, Schall K, Ramirez SH, Persidsky Y. Activation of protein tyrosine kinases and matrix metalloproteinases causes blood–brain barrier injury: novel mechanism for neurodegeneration associated with alcohol abuse. Glia 2008b;56:78–88. [PubMed: 17943953]

Harper C. The neuropathology of alcohol-specific brain damage, or does alcohol damage the brain? J Neuropathol Exp Neurol 1998;57:101–110. [PubMed: 9600202]

Harper C, Dixon G, Sheedy D, Garrick T. Neuropathological alterations in alcoholic brains. Studies arising from the New South Wales Tissue Resource Centre. Prog Neuropsychopharmacol Biol Psychiatry 2003;27:951–961. [PubMed: 14499312]

Hawkins BT, Egleton RD. Fluorescence imaging of blood–brain barrier disruption. J Neurosci Methods 2006;151:262–267. [PubMed: 16181683]

Kessova IG, Cederbaum AI. Mitochondrial alterations in livers of Sod1−/− mice fed alcohol. Free Radic Biol Med 2007;42:1470–1480. [PubMed: 17448893]

Kido Y, Tamai I, Ohnari A, Sai Y, Kagami T, Nezu J, Nikaido H, Hashimoto N, Asano M, Tsuji A. Functional relevance of carnitine transporter OCTN2 to brain distribution of L-carnitine and acetyl-L-carnitine across the blood–brain barrier. J Neurochem 2001;79:959–969. [PubMed: 11739607]

Leybaert L. Neurobarrier coupling in the brain: a partner of neurovascular and neurometabolic coupling? J Cereb Blood Flow Metab 2005;25:2–16. [PubMed: 15678108]

Lin MT, Beal MF. Mitochondrial dysfunction and oxidative stress in neurodegenerative diseases. Nature 2006;443:787–795. [PubMed: 17051205]

Lolic MM, Fiskum G, Rosenthal RE. Neuroprotective effects of acetyl-L-carnitine after stroke in rats. Ann Emerg Med 1997;29:758–765. [PubMed: 9174521]

Lund-Andersen H, Kjeldsen CS, Hertz L, Brondsted HE. Uptake of glucose analogues by rat brain cortex slices: Na+-independent membrane transport. J Neurochem 1976;27:369–373. [PubMed: 965977]

Maher F, Vannucci SJ, Simpson IA. Glucose transporter proteins in brain. FASEB J 1994;8:1003–1011. [PubMed: 7926364]

Maracchioni A, Totaro A, Angelini DF, Di Penta A, Bernardi G, Carri MT, Achsel T. Mitochondrial damage modulates alternative splicing in neuronal cells: implications for neurodegeneration. J Neurochem 2007;100:142–153. [PubMed: 17064354]

Oscar-Berman M, Marinkovic K. Alcoholism and the brain: an overview. Alcohol Res Health 2003;27:125–133. [PubMed: 15303622]

Pardridge, WM.; Boado, RJ. The blood–brain barrier. Pardridge, WM., editor. Raven; New York: 1993. p. 395-440.

Parsons OA. Neurocognitive deficits in alcoholics and social drinkers: a continuum? Alcohol Clin Exp Res 1998;22:954–961. [PubMed: 9660328]

Pastorino JG, Marcineviciute A, Cahill A, Hoek JB. Potentiation by chronic ethanol treatment of the mitochondrial permeability transition. Biochem Biophys Res Commun 1999;265:405–409. [PubMed: 10558880]

Pettegrew JW, Klunk WE, Panchalingam K, Kanfer JN, McClure RJ. Clinical and neurochemical effects of acetyl-L-carnitine in Alzheimer's disease. Neurobiol Aging 1995;16:1–4. [PubMed: 7723928]

Rump TJ, Muneer PM, Szlachetka A, Lamb A, Haorei C, Alikunju S, Xiong H, Keblesh J, Liu J, Zimmerman MC, Jones J, Donohue TM Jr, Persidsky Y, Haorah J. Acetyl-L-carnitine protects neuronal function from alcohol-induced oxidative damage in the brain. Free Radic Biol Med 2010;49:1494–1504. doi:10.1016/j.freeradbiomed.2010.08.011. [PubMed: 20708681]

Singh SP, Snyder AK, Eman S. Effects of ethanol on hexose uptake by cultured rat brain cells. Alcohol Clin Exp Res 2006;14:741–745. [PubMed: 2264604]

Takakura Y, Kuentzel SL, Raub TJ, Davies A, Baldwin SA, Borchardt RT. Hexose uptake in primary cultures of bovine brain microvessel endothelial cells. I. Basic characteristics and effects of D-glucose and insulin. Biochim Biophys Acta 1991;1070:1–10. [PubMed: 1751515]

Volkow ND, Wang GJ, Franceschi D, Fowler JS, Thanos PP, Maynard L, Gatley SJ, Wong C, Veech RL, Kunos G, Kai Li T. Low doses of alcohol substantially decrease glucose metabolism in the human brain. Neuroimage 2006;29:295–301. [PubMed: 16085426]

WHO. WHO Statistical Information System (WHOSIS); Geneva: 2007.

Yeh WL, Lin CJ, Fu WM. Enhancement of glucose transporter expression of brain endothelial cells by vascular endothelial growth factor derived from glioma exposed to hypoxia. Mol Pharmacol 2008;73:170–177. [PubMed: 17942749]

Zeigler DW, Wang CC, Yoast RA, Dickinson BD, McCaffree MA, Robinowitz CB, Sterling ML. The neurocognitive effects of alcohol on adolescents and college students. Prev Med 2005;40:23–32. [PubMed: 15530577]

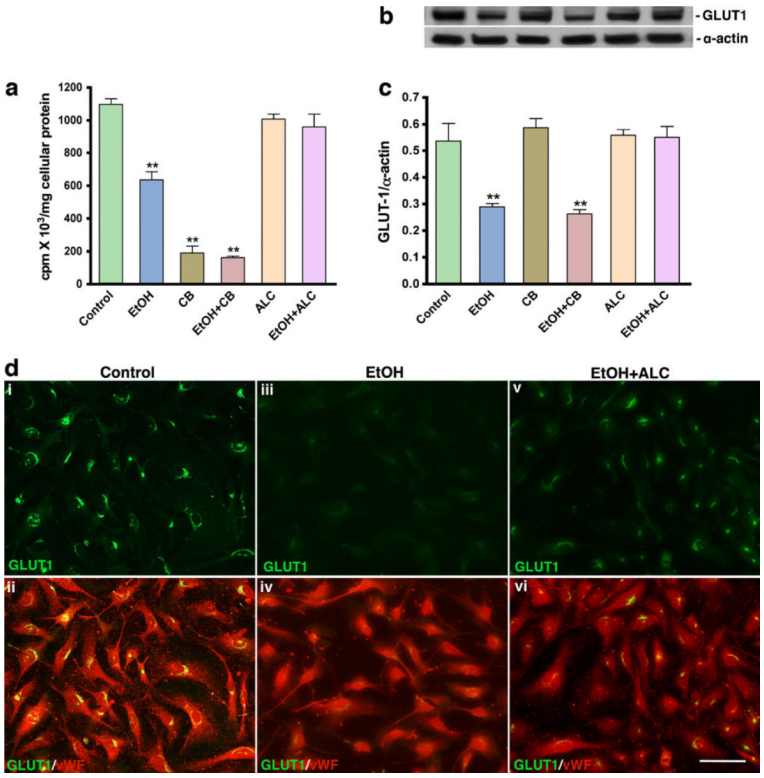

Fig. 1.

Inhibitory effects EtOH on glucose uptake and GLUT1 expression in human BECs: **a** effect of EtOH on D-(2-^{3}H)-glucose uptake in human BECs with or without GLUT1 inhibitor cytochalasin B(*CB*; 10 μM) or acetyl-L-carnitine (ALC; 200 μM). **b** Effect of EtOH on 55-kDa isoform GLUT1 protein levels in hBECs by Western blot analysis. c Results are expressed as the ratio of GLUT1 to α-actin bands and presented as mean values (± SD; *n*=4). *d* Immunocytochemistry of GLUT1 (green) merged with von Willebrand factor (*vWF*; red) is shown in control (*i, ii*), 50 mM EtOH (iii, iv), and EtOH + ALC (*v, vi*) treated human BECs. ***p*<0.01 statistically significant compared with control. Scale bar indicates 20 μm in the panels of **d**

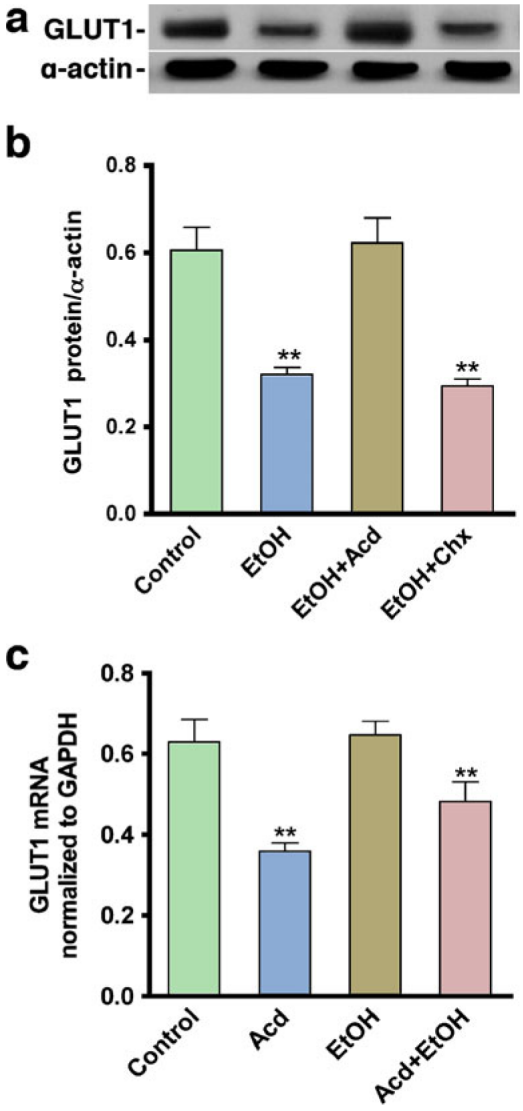

Fig. 2.

The regulation of GLUT1 expression is in translation level: (**a–b**) Analysis of the regulation of GLUT1 expression by treating actinomycin D (*act*-D, transcription inhibitor, 100 ng/mL) and cycloheximide (*Chx*, translation inhibitor, 10 μg/mL) in 50 mM EtOH exposed human BECs. The results show the regulation of GLUT1 was affected at translation level. (**b**) Results are expressed as the ratio of GLUT1 to a-actin bands, and presented as mean values (± SD; *n*=3). (**c**) GLUT1 mRNA level normalized with GAPDH (± SD; *n*=3). **p<0.01 statistically significant compared with control

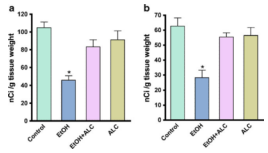

Fig. 3.

EtOH inhibits glucose uptake in animal model: effect of chronic EtOH administration (4%, v/v) on glucose uptake in vivo in cerebral cortex (**a**) and cerebellum (**b**). D-(2-^{3}H)-glucose (4 μCi) and non-radiolabeled glucose in 500 μlof saline were cavaged orally for control, EtOH, and EtOH + ALC animals. After 1 h, the mice were sacrificed and tissue processed for glucose uptake assay. *p<0.05 statistically significant compared with control

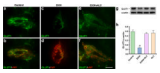

Fig. 4.

EtOH exposure impairs GLUT1 expression in brain microvessels: immunohistochemistry of GLUT1 (green) in microvessels merged with vWF (*red*) in control (**a, b**), EtOH (**c, d**), and EtOH + ALC (**e, f**). g Western blot analysis of 55-kDa isoform of GLUT1 protein in brain microvessels. h Results are expressed as the ratio of GLUT1 to α-actin bands and presented as mean values (± SD; *n*=3). **p<0.01 statistically significant compared with control. Scale bar indicated 20 μmin **a–f**

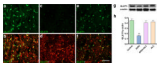

Fig. 5.

EtOH exposure impairs GLUT1 expression in brain tissues: immunohistochemistry of GLUT1 (*green*) in brain tissue sections merged with vWF (*red*) in control (**a, b**), EtOH (**c, d**), and EtOH + ALC (**e, f**).g Western blot analysis of 45-kDa isoform GLUT1 protein in brain tissue protein extract. h Results are expressed as the ratio of GLUT1 to α-actin bands and presented as mean values (± SD; n=3). **p<0.01 statistically significant compared with control. Scale bar indicated 20 μmin **a–f**

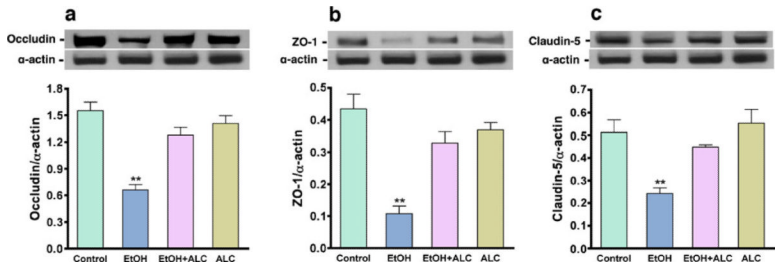

Fig. 6.

Effect of EtOH on tight junction (TJ) protein expression: Western blot analysis of TJ proteins such as (a) occludin (65 kDa), (b) ZO-1 (225 kDa), and (c) claudin-5 (23 kDa) are shown in control and EtOH, EtOH + ALC, and ALC exposed mice brain microvessels. *Bar* graphs show that the results are expressed as the ratio of occludin or claudin-5 or ZO-1 to α-actin bands and presented as mean values (± SD; $n=3$). $^{**}p<0.01$ statistically significant compared with control

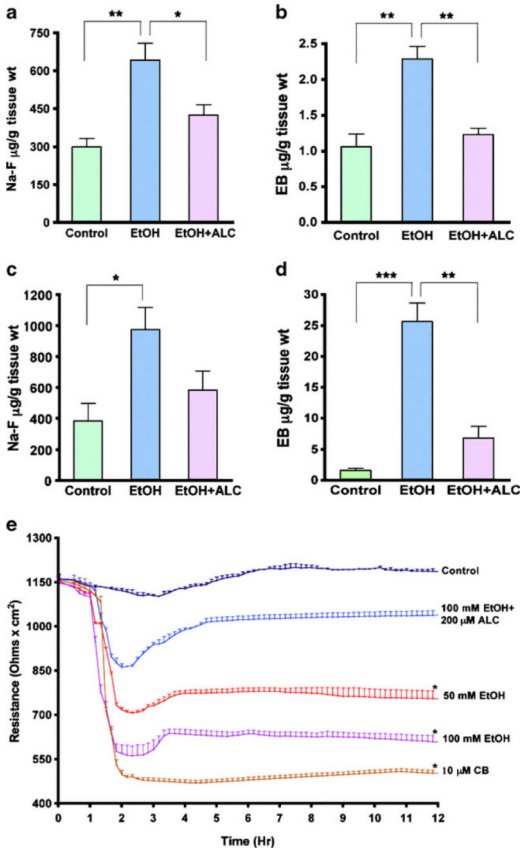

Fig. 7.

EtOH increases BBB permeability and decreases BBB electrical resistance: Permeability of sodium fluorescein (*NaFl; 5* µM)/Evans Blue (EB;5 µM) across the BBB is shown in a, b acute EtOH exposure (single dose of 650 mM) and c, d chronic EtOH administration (4%, *v/v*). e TEER of hBECs monolayers following treatment with various test compounds (n=3). TEER was measured at 400 Hz in 10-min intervals for 12 h. The treatments were started after stable resistance was reached for 2 h.*p<0.05, **p<0.01, and ***p<0.001 statistically significant compared with control

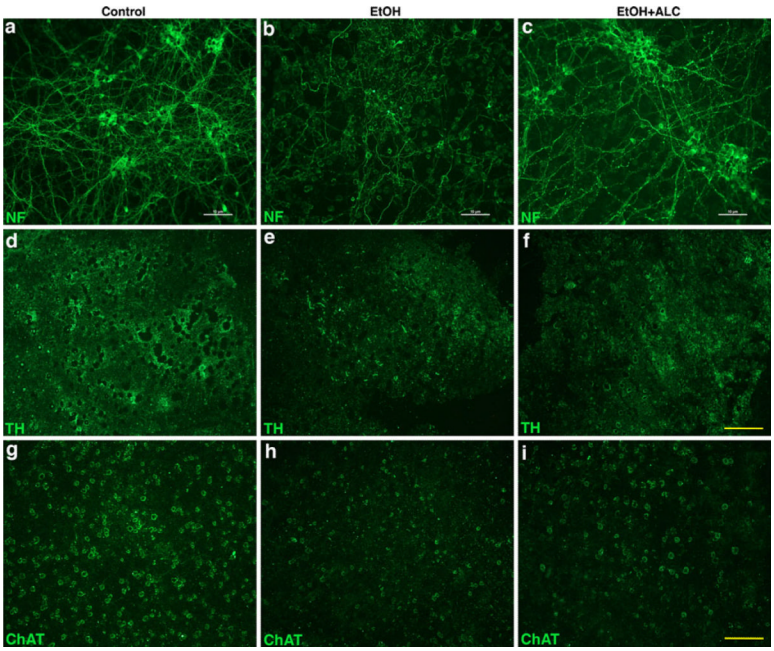

Fig. 8.

Loss of BBB integrity leads to neurodegeneration. a–c Primary human neurons cultured on glass cover slips (40,000 cells/well) were treated with 50 mM EtOH ± ALC for 48 h and were analyzed for the integrity of neurofilaments (*NF*; green)in a control, b EtOH, and c EtOH + ALC (ALC=200 μM). **d–f** Effect of chronic EtOH administration on dopaminergic neurons (the expression of dopaminergic neuronal marker, tyrosine hydroxylase (*TH*), green) and g–i on cholinergic neurons (the expression of cholinergic neuronal marker, choline acetyltransferase (*ChAT), green*) are shown in brain *cortical* tissue sections. *Scale* bar indicated 10 μmin a–c and 20 μmin d–i